

# Theory of spin torque due to spin-orbit coupling

A. Manchon and S. Zhang

*Department of Physics, University of Arizona, Tucson, Arizona 85721, USA*

(Received 23 December 2008; published 23 March 2009; publisher error corrected 30 March 2009)

The combined effect of spin-orbit coupling and exchange interaction in a single ferromagnetic layer is investigated. It is shown that, in nonequilibrium regime, the spin-orbit interaction (SOI) gives rise to a transverse spin density that exerts a torque on the local magnetization. The spin torque depends on the symmetry properties of the SOI. For the inversion-symmetry-preserved SOI such as the impurity SOI and the Luttinger spin-orbit band, the spin torque is a high-order effect too small to lead to a reasonable critical switching current density. For the inversion-symmetry-broken SOI, e.g., Rashba and Dresselhaus SOIs, the torque is on the first order of the SOI parameter and can be effectively used to control the magnetization direction using critical switching current densities as low as  $10^4$ – $10^6$  A/cm<sup>2</sup>. We also address the relation between the spin torque and the anisotropic magnetoresistance. Finally, a number of systems are proposed for the experimental observation of the SOI-induced torque.

DOI: [10.1103/PhysRevB.79.094422](https://doi.org/10.1103/PhysRevB.79.094422)

PACS number(s): 75.60.Jk, 75.75.+a, 72.25.-b, 72.10.-d

## I. INTRODUCTION

Manipulating the magnetization direction of a ferromagnet without the use of an external magnetic field has been made possible by the theoretical prediction of the spin-transfer torque (STT) effect by Slonczewski<sup>1</sup> and Berger<sup>2</sup> in 1996. The STT, which is now usually observed in metallic<sup>3</sup> and tunneling spin valves,<sup>4</sup> as well as magnetic domain walls,<sup>5</sup> comes from the transfer of the transverse spin current of conduction electrons to the background magnetization and requires the noncollinear configuration of the magnetic structure. In these studies, the spin-orbit interaction (SOI) is usually considered unimportant in the role of the spin transfer.

However, the importance of SOI has been emphasized in other studies, for example, the experimental and theoretical researches of anisotropic magnetoresistance (AMR),<sup>6</sup> anomalous Hall effect (AHE),<sup>7</sup> and spin Hall effect (SHE).<sup>8</sup> It is only recently that the effect of the spin-orbit coupling on the spin torque has been considered in the domain-wall motion.<sup>9,10</sup>

We have<sup>11</sup> proposed that by using the Rashba SOI along with the ferromagnetic exchange interaction, the electric current can induce a spin torque on the magnetization even in a *uniformly magnetized single layer*, without any noncollinearity of the magnetization. Physically, the Rashba SOI creates a nonequilibrium spin density whose direction is perpendicular to the current flow and to the potential confinement (normal to the layer). The nonequilibrium spin density interacts with the magnetization via the ferromagnetic exchange coupling and ultimately rotates the magnetization for a sufficiently high current density. Thus, the torque generated by the Rashba SOI is equivalent to an effective magnetic field; this is very different from the STT which involves the transfer of the spin current.<sup>11</sup>

In the present paper, we extend our study of the current-induced spin torque in other spin-orbit coupled systems. We find that the different forms of the SOI give rise to different orders of magnitude of the spin torque, depending on the symmetry of the interaction. For some forms of the SOI, we show that the spin torque only exists in the higher orders

with respect to the spin-orbit coupling parameter. Since we are interested in torques that can induce magnetization switching for reasonable critical current densities ( $<10^7$  A/cm<sup>2</sup>), we will only focus on first-order terms and will not explicitly calculate the form of higher-order components.

The paper is organized as follows. In Sec. II, we present the principle of such a torque based on the spin continuity equation. We also propose a simple physical picture to understand the combined effect of exchange interaction and SOI. The spin torque is then investigated for different forms of the spin-orbit interaction in Sec. III. After discussing the case of three-dimensional systems we derive the form of the torque for two-dimensional systems with Rashba and Dresselhaus spin-orbit couplings. In Sec. IV, we first sum up our results by emphasizing the importance of the SOI symmetries and address the relation between the AMR and the SOI-induced torque in the different cases. We then stress out the differences between the usual STT and our SOI-induced torque and finally discuss the experimental observation of such a torque. The conclusion is given in Sec. V.

## II. PRINCIPLE OF SPIN-ORBIT-INDUCED TORQUE

The coupling between the electron spin and its orbital can be derived from the Dirac equation for a relativistic electron, expanded to the lowest order in  $(v/c)^2$  ( $v$  and  $c$  are the electron and light velocities, respectively). In a ferromagnetic layer in the presence of spin-orbit coupling, the one-particle Hamiltonian is

$$\hat{H} = \hat{H}_0 + \hat{H}_{\text{so}}, \quad (1)$$

$$\hat{H}_0 = \frac{\hat{\mathbf{p}}^2}{2m} - J_{\text{ex}} \hat{\mathbf{M}} \cdot \hat{\boldsymbol{\sigma}}, \quad (2)$$

$$\hat{H}_{\text{so}} = \frac{\hbar}{2mc^2} (\nabla V \times \hat{\mathbf{p}}) \cdot \hat{\boldsymbol{\sigma}}, \quad (3)$$

where  $m$  is the carrier mass,  $\hbar$  is the reduced Planck's constant, and  $c$  is the light velocity.  $\hat{H}_0$  represents the free-

electron Hamiltonian in a ferromagnetic layer with magnetization direction  $\hat{\mathbf{M}}$  and with an exchange coupling  $J_{\text{ex}}$  between the carriers' spin and the background magnetization.  $\hat{\sigma}$  is the operator of Pauli-spin matrices.  $\hat{H}_{\text{so}}$  represents the interaction between the carrier spin and the carrier momentum.  $\nabla V$  is the effective local electric field seen by the itinerant charge with momentum operator  $\hat{\mathbf{p}}$ . As we will see in Sec. III, this potential arises from different sources, such as impurities, host atoms, as well as the structural confinement. We will consider a set of commonly used forms of spin-orbit coupling later.

From the above Hamiltonian, we can deduce the spin-density continuity equation for carriers and find

$$\frac{d\mathbf{m}}{dt} = -\nabla \cdot \mathcal{J}_s - \frac{J_{\text{ex}}}{\hbar} \mathbf{M} \times \mathbf{m} + \frac{1}{2mc^2} \langle (\nabla V \times \hat{\mathbf{p}}) \times \hat{\sigma} \rangle, \quad (4)$$

where  $\mathbf{m} = \langle \hat{\sigma} \rangle$  is the spin density and  $\mathcal{J}_s$  is the spin current tensor.  $\langle \cdots \rangle$  denotes quantum-mechanical averaging. In the above equation of motion, we have treated the local magnetization vector  $\mathbf{M}$  classically. The equation of motion for this classical vector  $\mathbf{M}$  is usually modeled by the Landau-Lifshitz-Gilbert equation in addition to the spin torque due to the presence of the nonequilibrium spin density  $\mathbf{m}$ ,

$$\frac{d\mathbf{M}}{dt} = -\gamma \mathbf{M} \times \mathbf{H} + \eta \mathbf{M} \times \frac{d\mathbf{M}}{dt} + \frac{J_{\text{ex}}}{\hbar} \mathbf{M} \times \mathbf{m}, \quad (5)$$

where  $\mathbf{H}$  is the effective field,  $\gamma$  is the gyromagnetic ratio, and  $\eta$  is the Gilbert damping. The last term is called the current-induced spin torque  $\mathbf{T}$ , which is the subject of our calculations throughout the paper. Assuming a uniformly magnetized single layer ( $\nabla \cdot \mathcal{J}_s = 0$ ) in steady-state ( $d/dt = 0$ ) condition, the out-of-equilibrium torque on the magnetization is directly proportional to the spin density of the conduction electrons,

$$\mathbf{T} \equiv \frac{J_{\text{ex}}}{\hbar} \mathbf{M} \times \mathbf{m} = \frac{1}{2mc^2} \langle (\nabla V \times \hat{\mathbf{p}}) \times \hat{\sigma} \rangle. \quad (6)$$

Before we calculate Eq. (6) for various spin-orbit interactions in the nonequilibrium condition, we consider a simple case where the gradient of the potential in the spin-orbit Hamiltonian is replaced with a constant vector in the direction normal to the layer  $\mathbf{z}$ , i.e.,  $\nabla V \propto \mathbf{z}$ . This is known as the Rashba Hamiltonian<sup>12</sup> and it is derived for the structure inversion-asymmetric systems; we will further discuss the Rashba Hamiltonian in Secs. III and IV. In this case, the spin torque of Eq. (6) becomes

$$\mathbf{T} = \frac{\alpha}{\hbar} \langle (\hat{\mathbf{z}} \times \hat{\mathbf{p}}) \times \hat{\sigma} \rangle. \quad (7)$$

To see how the above spin torque is estimated in the presence of the electric field, we illustrate the Fermi surfaces for three cases. First, consider a ferromagnet *without* spin-orbit coupling, the Fermi surfaces of majority and minority bands are for the carrier spins pointing parallel and antiparallel to the magnetization [see Fig. 1(a)]. When applying an electric field, the Fermi surface of each band is shifted [dashed

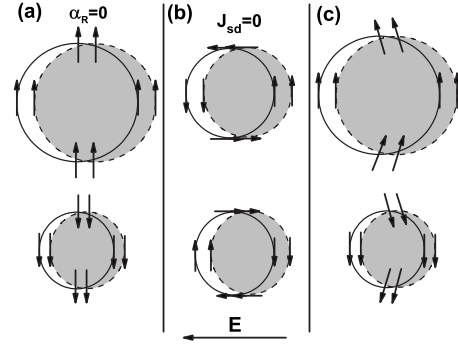


FIG. 1. Schematics of the Fermi surface for majority (top) and minority (bottom) electrons (a) in a ferromagnet without Rashba SOI, (b) in a layer with Rashba SOI and without exchange interaction, and (c) in a ferromagnet with small Rashba SOI.

circles in Fig. 1(a)], but the amount of spins in excess is exactly balanced by the amount of lacking spins. The net spin density generated by the Fermi-surface shift for both spin populations is then zero, i.e., there is no nonequilibrium spin density and thus the spin torque is zero.

In the second case where there is only spin-orbit coupling but without exchange interaction between the background magnetization and the itinerant spins, the Fermi surfaces are two spheres with the spin direction perpendicular to the electron momentum. When the electric field displaces the Fermi surfaces in the direction of the current [see Fig. 1(b)], each band gains a net spin density with an opposite sign. Since these two Fermi spheres have different radius, the total spin density is thus finite. However, these electric-field-induced spin densities do not exert a torque the local magnetization due to the absence of the exchange interaction.

Thus one needs both SOI and the exchange interaction to generate the current-driven spin torque. The Rashba SOI produces the nonequilibrium spin density proportional to the current density and the exchange interaction couples the electron-spin density with the local magnetization. Figure 1(c) shows the spin configuration on the Fermi surface when the Rashba SOI is small compared to the exchange interaction. The detailed spin configuration depends on the form of the SOI; we will discuss the various SOIs next.

### III. SPIN TORQUES FOR VARIOUS SPIN-ORBIT INTERACTIONS

While Eq. (3) is the general form of the SOI coupling, the potential  $V$  in Eq. (3) includes all electric potentials in the solids. In this section, we consider several special forms which have been frequently used in model calculations for AMR, AHE, and SHE. First, we analyze the impurity-induced SOI in three-dimensional systems. Then, we will study the spin torque for Luttinger SOI. In both cases, we find the spin torque vanishes for the first order of the spin-orbit coupling parameter; thus, the spin torque is a high-order effect. Finally, we consider the SOI with bulk and structure inversion asymmetries<sup>12,13</sup> and find that the spin torque exists in the first order of the spin-orbit coupling.

### A. Impurity spin-orbit interaction

In bulk ferromagnetic systems, the SOI has two origins: intrinsic (related to the band structure of the host elements) and extrinsic (related to the impurities). They both contribute to the spin asymmetry in the electronic transport, giving rise to AMR, AHE, and SHE. The extrinsic SOI gives rise to both an anomalous velocity<sup>14</sup> (extrinsic skew scattering) and to a displacement in the electron average position<sup>15,16</sup> (side jump scattering). We consider below the spin torque for the impurity SOI.

The impurity Hamiltonian including the spin-orbit interaction is

$$\hat{H}_{\text{imp}} = \sum_j V(\mathbf{r} - \mathbf{R}_j) + \frac{\lambda_{\text{so}}}{\hbar} (\nabla V(\mathbf{r} - \mathbf{R}_j) \times \hat{\mathbf{p}}) \cdot \hat{\boldsymbol{\sigma}}, \quad (8)$$

where  $V(\mathbf{r} - \mathbf{R}_j)$  is the potential of the impurity  $\mathbf{R}_j$  and  $\lambda_{\text{so}}$  is the spin-orbit coupling parameter. It is noted that  $\lambda_{\text{so}}$  is usually a factor of 1000 larger than the bare spin-orbit parameter ( $\hbar^2/2mc^2$ ) due to the influence of Bloch states.<sup>17</sup>

The treatment of spin transport for the above impurity SOI has been carried out, for instance, by Potter<sup>18</sup> to address the issue of AMR and by Crepieux and Bruno<sup>16</sup> to study the AHE. These treatments required either second- or third-order perturbation theory and yielded effects proportional to at least  $\lambda_{\text{so}}^2$ . Performing a similar calculation, we show that the spin torque up to first order of  $\lambda_{\text{so}}$  vanishes as well.

The Fourier transform of the above Hamiltonian is

$$\hat{H}_{\text{imp}} = \sum_j \sum_{\mathbf{k}'} V_{\mathbf{k}\mathbf{k}'} e^{i(\mathbf{k}-\mathbf{k}')(\mathbf{r}-\mathbf{R}_j)} \left\{ 1 + i \frac{\lambda_{\text{so}}}{\hbar} [(\mathbf{k} - \mathbf{k}') \times \hat{\mathbf{p}}] \cdot \hat{\boldsymbol{\sigma}} \right\}. \quad (9)$$

The scattering states are described using the Lippman-Schwinger equation

$$|\mathbf{k}, s\rangle_{\text{sc}} = |\mathbf{k}, s\rangle_0 + \frac{1}{\epsilon_k^s - H_0 + i0} H_{\text{imp}} |\mathbf{k}, s\rangle_{\text{sc}}. \quad (10)$$

This state can be developed up to the desired order to obtain the anisotropic effect within the conductance and the spin accumulation. The scattering rate is then obtained from the usual Fermi golden rule,

$$W_{kk'}^{ss'} = \frac{2\pi}{\hbar} \sum_j |{}_{\text{sc}}\langle \mathbf{k}, s | V(\mathbf{r} - \mathbf{R}_j) | \mathbf{k}', s' \rangle_{\text{sc}}|^2 \delta(\epsilon_k^s - \epsilon_{k'}^{s'}). \quad (11)$$

Up to the second order in the impurity potential, assuming that  $V(\mathbf{r}) \approx V\delta(\mathbf{r})$ , the relaxation rate reads

$$W_{kk}^{ss} \approx \frac{2\pi N |V|^2}{\hbar} \delta_{ss'} (1 + 8\pi^2 |V|^2 \sum_{k'', s''} \delta(\epsilon_k^s - \epsilon_{k''}^{s''}) \times (\delta_{ss''} + \lambda_{\text{so}}^2 [k \times k''] \cdot \boldsymbol{\sigma}_{ss''}) [(k \times k'') \cdot \boldsymbol{\sigma}_{s''s'}]), \quad (12)$$

where  $N$  is the impurity concentration and  $\epsilon_k^s$  is the electron energy. The anisotropic magnetoresistance can be obtained using the Boltzmann formalism. By using an unperturbed

electron velocity  $\mathbf{v} = \hbar \mathbf{k} / m$  (the anisotropic scattering essentially lies in the scattering rate<sup>6</sup>), we find that the AMR is on the form  $\propto \lambda_{\text{so}}^2 |V|^2$ . To calculate the spin torque, we use Eq. (6) as follows:

$$\mathbf{T}_k^s = \frac{\lambda_{\text{so}}}{\hbar} {}_{\text{sc}}\langle k, s | (\nabla V(\mathbf{r}) \times \hat{\mathbf{p}}) \cdot \hat{\boldsymbol{\sigma}} | k, s \rangle_{\text{sc}}. \quad (13)$$

Up to the second order in the impurity potential and the first order in  $\lambda_{\text{so}}$ , the spin torque is

$$\mathbf{T}_k^s = 4\pi N \lambda_{\text{so}} \sum_{k', s'} \delta(\epsilon_k^s - \epsilon_{k'}^{s'}) |V_{\mathbf{k}\mathbf{k}'}|^2 (\mathbf{k} \times \mathbf{k}') \times \boldsymbol{\sigma}_{ss'}. \quad (14)$$

As long as the potential  $V_{\mathbf{k}\mathbf{k}'}$  is an even function of  $\mathbf{k} - \mathbf{k}'$ , the spin torque is zero when we integrate  $\mathbf{k}'$  in Eq. (14). We conclude that the spin torque vanishes up to the first order in the impurity spin-orbit parameter. The calculation of the spin torque to the second order is rather cumbersome; we will not give the explicit expression here.

### B. Luttinger spin-orbit Hamiltonian

A number of III-V Mn-doped semiconductors are known to become ferromagnetic at low temperature,<sup>19</sup> e.g., (In,Mn)As, (Ga,Mn)As, or (Ga,Mn)N, due to the coupling between Mn impurities mediated by the holes.<sup>20</sup> The band structure of these materials shows fourfold degenerates at the  $K$  point of the valence bands, usually modeled by the Luttinger Hamiltonian.<sup>21</sup> Thus our effective Hamiltonian consists of the Luttinger Hamiltonian  $\hat{H}_L$  of  $s=3/2$  holes and the exchange interaction,

$$\hat{H} = \hat{H}_L - J_{\text{pd}} \hat{\mathbf{s}} \cdot \hat{\mathbf{M}}, \quad (15)$$

where  $J_{\text{pd}}$  is the effective exchange energy between the Mn cations and the itinerant  $p$ -type holes, such that  $J_{\text{pd}} = J_i N_{\text{Mn}} S_{\text{Mn}}$ , where  $J_i$  is the exchange integral,  $N_{\text{Mn}}$  is the concentration of the Mn cations, and  $S_{\text{Mn}} = 5/2$  is the spin of the acceptors.<sup>20</sup> The magnetization direction of the Mn impurities is  $\hat{\mathbf{M}} = \hat{\mathbf{z}}$ . The Luttinger Hamiltonian in Eq. (15) is defined as

$$\hat{H}_L = \frac{\hbar^2}{2m} \left[ \left( \gamma_1 + \frac{5}{2} \gamma_2 \right) k^2 - 2\gamma_2 (\mathbf{k} \cdot \hat{\mathbf{J}})^2 \right] \quad (16)$$

and  $\hat{\mathbf{J}} = \hat{\mathbf{r}} \times \hat{\mathbf{p}} + \hat{\mathbf{s}}$  is the total angular-momentum operator. Note that the spin operator  $\hat{\mathbf{s}}$  for  $3/2$  spins is now a  $6 \times 6$  matrix accounting for heavy holes, light holes, and split-off bands (see Ref. 22 for example). In the following, we neglect the role of the split-off bands and focus on heavy holes and light holes, reducing the Hamiltonian (16) to a  $4 \times 4$  matrix. We explicitly show below that the spin torque vanishes in the first order of the spin-orbit coupling parameter for both strong- and weak-coupling limits.

#### 1. Weak spin-orbit coupling

We first examine the weak spin-orbit coupling, i.e.,  $\gamma_2 \ll \gamma_1, J_{\text{pd}} / \epsilon_F$  ( $\epsilon_F$  is the Fermi energy). In this limiting case,

we assume that the orbital angular momentum is negligible so that the total angular momentum essentially reduces to the spin angular momentum. Then, the unperturbed Hamiltonian  $\hat{H}_0 = \gamma_1 \hat{\mathbf{p}}^2 / 2m - J_{\text{pd}} \hat{s}_z$  has four nondegenerate eigenstates and eigenenergies for the fixed wave vector  $\mathbf{k}$ ,

$$|hh, \uparrow(\downarrow)\rangle, \quad \epsilon_{hh}^{\uparrow(\downarrow)} = \gamma_1 \hbar^2 k^2 / 2m \mp J_{\text{pd}} / 2, \quad (17)$$

$$|lh, \uparrow(\downarrow)\rangle, \quad \epsilon_{lh}^{\uparrow(\downarrow)} = \gamma_1 \hbar^2 k^2 / 2m \mp J_{\text{pd}} / 6. \quad (18)$$

Here,  $\epsilon_{hh}$  and  $\epsilon_{lh}$  is a notation that does not necessarily refer to heavy and light holes. Using the first-order perturbation theory, up to the first order in up to the first order in  $\gamma_2$ , the eigenstates are

$$|hh, +\rangle = |hh, \uparrow\rangle + \frac{3\sqrt{3}\gamma_2 \hbar^2 k^2}{J_{\text{pd}} 2m} \left( 0, \frac{\sin^2 \varphi}{2} e^{2i\phi}, \sin 2\varphi e^{i\phi}, 0 \right)^T, \quad (19)$$

$$|hh, -\rangle = |hh, \downarrow\rangle - \frac{3\sqrt{3}\gamma_2 \hbar^2 k^2}{J_{\text{pd}} 2m} \left( 0, \sin 2\varphi e^{-i\phi}, \frac{\sin^2 \varphi}{2} e^{-2i\phi}, 0 \right)^T, \quad (20)$$

$$|lh, +\rangle = |lh, \uparrow\rangle + \frac{3\sqrt{3}\gamma_2 \hbar^2 k^2}{J_{\text{pd}} 2m} \left( \sin 2\varphi e^{-i\phi}, 0, 0, -\frac{\sin^2 \varphi}{2} e^{2i\phi} \right)^T, \quad (21)$$

$$|lh, -\rangle = |lh, \downarrow\rangle - \frac{3\sqrt{3}\gamma_2 \hbar^2 k^2}{J_{\text{pd}} 2m} \left( \sin 2\varphi e^{i\phi}, 0, 0, \frac{\sin^2 \varphi}{2} e^{-2i\phi} \right)^T, \quad (22)$$

where the superscript  $T$  denotes the matrix transposition and  $\mathbf{k} = k(\sin \varphi \cos \phi, \sin \varphi \sin \phi, \cos \varphi)$ . Thus the transverse spin densities of these states are

$$\langle \sigma_+ \rangle_{hh}^+ = \langle \sigma_+ \rangle_{hh}^- = \frac{3\gamma_2 \hbar^2 k^2}{J_{\text{pd}} 2m} \sin 2\varphi e^{i\phi}, \quad (23)$$

$$\langle \sigma_+ \rangle_{lh}^+ = \langle \sigma_+ \rangle_{lh}^- = -\frac{3\gamma_2 \hbar^2 k^2}{J_{\text{pd}} 2m} \sin 2\varphi e^{i\phi}. \quad (24)$$

Within the Boltzmann formalism, the nonequilibrium transverse spin density is then

$$\mathbf{m} = -eE\tau_0 \sum_{j,s} \int \frac{d^3 \mathbf{k}}{(2\pi)^3} \langle \sigma_+ \rangle_j^s v_i \delta(\epsilon_j^s - \epsilon_F), \quad (25)$$

where the electric field  $E$  is applied along the direction  $i = \{x, y, z\}$ ,  $j = \{hh, lh\}$ ,  $s = \pm$ ,  $\tau_0$  is the relaxation time, and the electron velocity is  $v_i = \gamma_1 \hbar k_i / m$ . As expected, the transverse spin density vanishes after integration over  $\mathbf{k}$ , for both heavy holes and light holes, and thus there is no spin torque up to the first order in  $\gamma_2$ .

## 2. Strong spin-orbit coupling

In the opposite limit where  $\gamma_1, \gamma_2 \gg J_{\text{pd}} / \epsilon_F$ , we treat  $\hat{H}' = -J_{\text{pd}} \hat{s} \cdot \hat{\mathbf{M}}$  as a perturbation. In the following, we consider only the spin torque arising from heavy holes since the spin transport in DMS is generally dominated by these holes.<sup>20</sup> The eigenenergies of the unperturbed Luttinger Hamiltonian are  $\epsilon_L = \frac{\hbar^2 k^2}{2m} (\gamma_1 - 2\gamma_2)$  for heavy holes and the corresponding eigenstates are

$$|+\rangle = 1/2(e^{-2i\phi} \sin \varphi, \sqrt{3} \sin \varphi, 0, -2e^{i\phi} \cos \varphi), \quad (26)$$

$$|-\rangle = 1/2(2e^{-i\phi} \cos \varphi, 0, \sqrt{3} \sin \varphi, e^{2i\phi} \sin \varphi). \quad (27)$$

When the exchange interaction  $\hat{H}'$  is turned on as a perturbation, the first-order correction to the energy is  $\Delta \epsilon^s = sJ_{\text{pd}}/2 \cos(\phi - \theta) \sin \varphi$  and the eigenstates become

$$|\xi^+\rangle = \left( e^{-2i\phi} \cos^3 \frac{\varphi}{2}, \sqrt{3} \sin^2 \frac{\varphi}{2} \cos \frac{\varphi}{2}, \sqrt{3} e^{-i\phi} \cos^2 \frac{\varphi}{2} \times \sin \frac{\varphi}{2}, e^{i\phi} \sin^3 \frac{\varphi}{2} \right)^T, \quad (28)$$

$$|\xi^-\rangle = \left( e^{-2i\phi} \sin^3 \frac{\varphi}{2}, \sqrt{3} \cos^2 \frac{\varphi}{2} \sin \frac{\varphi}{2}, -\sqrt{3} e^{-i\phi} \sin^2 \frac{\varphi}{2} \cos \frac{\varphi}{2}, -e^{i\phi} \cos^3 \frac{\varphi}{2} \right)^T. \quad (29)$$

The spin density for these wave functions is thus

$$\mathbf{m} = \langle \hat{\boldsymbol{\sigma}} \rangle = s\mathbf{k}/2k, \quad (30)$$

i.e., the spin densities for majority and minority heavy holes are opposite and equal, so that no effective torque is generated by the first-order term in  $J_{\text{pd}}$ . One has to develop the perturbation theory one step further to obtain a spin torque. Consequently, the SOI-induced torque arising from the Luttinger band for the hole-mediated systems is not expected to produce magnetization switching at a reasonable current density.

## C. Inversion asymmetry

There are a number of systems in solids that do not have spatial inversion symmetries, i.e., the potential  $V(-\mathbf{r}) \neq V(\mathbf{r})$ . In these cases, the spin-orbit Hamiltonian [Eq. (3)] is not invariant under the spatial inversion. We discuss three commonly studied systems. First, if a crystal has a bulk inversion asymmetry (BIA), e.g., zinc-blende structure, such as GaAs or InSb, Dresselhaus<sup>13</sup> showed that the spin-orbit coupling has the following form:

$$\hat{H}_C = \gamma[k_x(k_y^2 - k_z^2)\sigma_x + k_y(k_z^2 - k_x^2)\sigma_y + k_z(k_x^2 - k_y^2)\sigma_z]. \quad (31)$$

When such a crystal is subjected to strain at the interface,<sup>23</sup> this introduces a structure inversion asymmetry (SIA) which yields a simpler form of the spin-orbit coupling as follows:

$$\hat{H}_D = \beta(\sigma_x k_x - \sigma_y k_y). \quad (32)$$

In the case of a thin layer embedded between two asymmetric interfaces, Bychkov and Rashba<sup>12</sup> introduced a different form of SIA spin-orbit coupling,

$$\hat{H}_R = \alpha(\hat{\mathbf{z}} \times \hat{\mathbf{k}}) \cdot \hat{\boldsymbol{\sigma}}. \quad (33)$$

The Rashba Hamiltonian postulates that the potential is highly dependent on the growth direction  $\hat{\mathbf{z}}$ , which is usually the case for the dimensional confinement potential in layered structures. An interesting characteristic of the SIA and BIA interactions is that they can be tuned by applying an external electric field across the two-dimensional electron gas (2DEG).<sup>24,25</sup>

The above three SOIs have been intensively studied both experimentally and theoretically. The relative amplitude of  $\alpha$ ,  $\beta$ , and  $\gamma$  is very material dependent and will be addressed in Sec. IV. We will first present the method we used to obtain the spin torque and then we will derive the spin torque in the presence of the  $k$ -linear Dresselhaus and Rashba SOIs. The case of cubic Dresselhaus effect will be addressed at the end of the section.

The Hamiltonian of a single ferromagnetic two-dimensional electron gas in the presence of both Rashba and Dresselhaus spin-orbit couplings is the combination of Eqs. (32) and (33),

$$\hat{H} = \hat{H}_0 + \alpha(\sigma_x k_y - \sigma_y k_x) + \beta(\sigma_x k_x - \sigma_y k_y), \quad (34)$$

where we confine the electron motion in two dimensions  $(x, y)$  and  $\hat{H}_0$  is defined by Eq. (2). We choose the magnetization direction at  $\hat{\mathbf{M}} = \cos \theta \hat{\mathbf{x}} + \sin \theta \hat{\mathbf{y}}$  and find that the electron eigenenergy and wave function are

$$\epsilon_{\mathbf{k}}^s = \frac{\hbar^2 k^2}{2m} + s \delta_{\mathbf{k}}, \quad (35)$$

$$\delta_{\mathbf{k}} = [(-J_{\text{sd}} \cos \theta + \alpha k_y + \beta k_x)^2 + (J_{\text{sd}} \sin \theta + \alpha k_x + \beta k_y)^2]^{1/2}, \quad (36)$$

and

$$\Psi_{\mathbf{k}}^s = \frac{1}{\sqrt{2A}} \begin{pmatrix} s e^{i\gamma_{\mathbf{k}}} \\ 1 \end{pmatrix} \exp(i\mathbf{k} \cdot \mathbf{r}), \quad (37)$$

where  $\tan \gamma_{\mathbf{k}} = (J_{\text{sd}} \sin \theta + \alpha k_x + \beta k_y) / (-J_{\text{sd}} \cos \theta + \alpha k_y + \beta k_x)$ ,  $s = \pm$ , and  $A$  is the area of the film. Then, the velocity and spin density are

$$\mathbf{v}_{\mathbf{k}}^s = \frac{\partial \epsilon_{\mathbf{k}}^s}{\hbar \partial \mathbf{k}} = \frac{\hbar \mathbf{k}}{m} + s \left( \frac{\beta}{\hbar} \cos \gamma_{\mathbf{k}} + \frac{\alpha}{\hbar} \sin \gamma_{\mathbf{k}} \right) \mathbf{x} + s \left( \frac{\beta}{\hbar} \sin \gamma_{\mathbf{k}} + \frac{\alpha}{\hbar} \cos \gamma_{\mathbf{k}} \right) \mathbf{y}, \quad (38)$$

$$\mathbf{m}^s = 2s e^{-i\gamma_{\mathbf{k}}}. \quad (39)$$

To calculate the nonequilibrium spin density and the spin torque in the presence of the current, we use the Boltzmann equation for the two bands,

$$e \mathbf{E} \cdot \mathbf{v}_{\mathbf{k}}^s \left( -\frac{\partial f_0^s}{\partial \epsilon_F} \right) = \sum_{s'} \int d^2 \mathbf{k}' W_{kk'}^{ss'} (f_{\mathbf{k}}^s - f_{\mathbf{k}'}^{s'}), \quad (40)$$

where  $\mathbf{E} = E(\cos \theta_0 \mathbf{x} + \sin \theta_0 \mathbf{y})$  is the electric field in the  $(x, y)$  plane,  $f_0^s$  is the equilibrium distribution of the two bands ( $s = \pm$ ), and the scattering probability is

$$W_{kk'}^{ss'} = \frac{2\pi}{\hbar} \sum_j |\langle \Psi_{\mathbf{k}}^s | V_{\text{sc}}(\mathbf{r} - \mathbf{R}_j) | \Psi_{\mathbf{k}'}^{s'} \rangle|^2 \delta(\epsilon_{\mathbf{k}}^s - \epsilon_{\mathbf{k}'}^{s'}) \\ = \frac{\pi n_i}{\hbar} V^2 [1 + ss' \cos(\gamma_{\mathbf{k}} - \gamma_{\mathbf{k}'})] \delta(\epsilon_{\mathbf{k}}^s - \epsilon_{\mathbf{k}'}^{s'}), \quad (41)$$

where  $V_{\text{sc}}(\mathbf{r}) = V \delta(\mathbf{r})$  is the impurity scattering potential,  $\mathbf{R}_j$  is the impurity position, and  $n_i$  is their concentration. The above definition accounts for both intra- ( $s = s'$ ) and interband ( $s = -s'$ ) scattering, so that Eq. (40) may be solved numerically.

However, Schliemann and Loss<sup>26</sup> proposed a formalism to exactly solve Eq. (40) in 2DEG provided that  $W_{kk'}^{ss'} = W_{k'k}^{s's}$ . The authors showed that the deviation from the equilibrium distribution  $g_{\mathbf{k}}^s = f_{\mathbf{k}}^s - f_0^s$  can be decomposed into longitudinal and transverse contributions  $g_{\mathbf{k}}^s = g_{\mathbf{k}}^{\parallel} + g_{\mathbf{k}}^{\perp}$  written as

$$g_{\mathbf{k}}^{\parallel} = -e \left( -\frac{\partial f_0^{\sigma}}{\partial \epsilon_F} \right) \frac{\tau_{\mathbf{k}}^{\parallel}}{1 + \left( \frac{\tau_{\mathbf{k}}^{\parallel}}{\tau_{\mathbf{k}}^{\perp}} \right)^2} \mathbf{E} \cdot \mathbf{v}_{\mathbf{k}}^s, \quad (42)$$

$$g_{\mathbf{k}}^{\perp} = -e \left( -\frac{\partial f_0^{\sigma}}{\partial \epsilon_F} \right) \frac{\tau_{\mathbf{k}}^{\perp}}{1 + \left( \frac{\tau_{\mathbf{k}}^{\perp}}{\tau_{\mathbf{k}}^{\parallel}} \right)^2} (\mathbf{z} \times \mathbf{E}) \cdot \mathbf{v}_{\mathbf{k}}^s. \quad (43)$$

The longitudinal and transverse relaxation times  $\tau_{\mathbf{k}}^{\parallel}$  and  $\tau_{\mathbf{k}}^{\perp}$  are

$$\tau_{\parallel}^s(\mathbf{k}) = \sum_{s'} \int \frac{d^2 \mathbf{k}'}{(2\pi)^2} W_{kk'}^{ss'} \left( 1 - \frac{|\mathbf{v}_{\mathbf{k}'}^{s'}|}{|\mathbf{v}_{\mathbf{k}}^s|} \cos(\vartheta_{\mathbf{k}}^s - \vartheta_{\mathbf{k}'}^{s'}) \right), \quad (44)$$

$$\tau_{\perp}^s(\mathbf{k}) = \sum_{s'} \int \frac{d^2 \mathbf{k}'}{(2\pi)^2} W_{kk'}^{ss'} \frac{|\mathbf{v}_{\mathbf{k}'}^{s'}|}{|\mathbf{v}_{\mathbf{k}}^s|} \sin(\vartheta_{\mathbf{k}}^s - \vartheta_{\mathbf{k}'}^{s'}), \quad (45)$$

and  $\cos \vartheta_{\mathbf{k}}^s = \mathbf{E} \cdot \mathbf{v}_{\mathbf{k}}^s / E |\mathbf{v}_{\mathbf{k}}^s|$  and  $\sin \vartheta_{\mathbf{k}}^s = (\mathbf{z} \times \mathbf{E}) \cdot \mathbf{v}_{\mathbf{k}}^s / E |\mathbf{v}_{\mathbf{k}}^s|$ . This method allows us to evaluate both currents and spin density in the general case.

### 1. Large exchange coupling

We assume that  $\epsilon_F \gg J_{\text{sd}} \gg \alpha k_F, \beta k_F$ , where  $k_F = \sqrt{2m\epsilon_F/\hbar^2}$ . Then, interband transitions can be neglected to a good approximation,<sup>11</sup> yielding an isotropic scattering probability  $W_{kk'}^{\sigma\sigma'} = \pi n_i V^2 / \hbar$  at the first order; this is equivalent to a constant relaxation-time approximation. Consequently, the Boltzmann distribution in Eq. (40) has a simple solution,

$$f_k^s = f_0^s - e\mathbf{E} \cdot \mathbf{v}_k^s \tau \left( -\frac{\partial f_0^s}{\partial E} \right), \quad (46)$$

where  $\tau$  is the relaxation time ( $e > 0$ ). The in-plane spin density is then

$$\begin{aligned} \mathbf{m}^s &= \sum_{\mathbf{k}} g_k^s \langle \Psi_{\mathbf{k}}^s | \hat{\sigma} | \Psi_{\mathbf{k}}^s \rangle \\ &= 2s \int \frac{d^2\mathbf{k}}{(2\pi)^2} g_k^s (\cos \gamma_k \mathbf{x} - \sin \gamma_k \mathbf{y}). \end{aligned} \quad (47)$$

The calculation is straightforward and we can rewrite the spin density  $\mathbf{m} = \mathbf{m}_{\parallel} + \mathbf{m}_{\perp}$ , where  $\mathbf{m}_{\parallel}$  is along the magnetization  $\mathbf{M}$  and  $\mathbf{m}_{\perp}$  is transverse to it. This yields

$$\mathbf{m}_{\parallel} = \frac{e\tau_0}{\pi} \frac{2m}{\hbar^3} [\alpha \sin(\theta - \theta_0) - \beta \cos(\theta + \theta_0)] \mathbf{M}, \quad (48)$$

$$\mathbf{m}_{\perp} = \frac{e\tau_0}{\pi} \frac{2m}{\hbar^3} [\alpha \cos(\theta - \theta_0) + \beta \sin(\theta + \theta_0)] \mathbf{M}_{\perp}, \quad (49)$$

where  $\mathbf{M}_{\perp} = \mathbf{M} \times \mathbf{z}$ . Then, the torque exerted on the local magnetization is

$$\mathbf{T} = \frac{J_{sd}}{\hbar} \mathbf{M} \times \mathbf{m} = 2J_e \frac{J_{sd}}{\epsilon_F} \frac{m}{e\hbar^2} [\alpha \cos(\theta - \theta_0) + \beta \sin(\theta + \theta_0)] \mathbf{z}, \quad (50)$$

where  $J_e = \sigma_0 E$  and  $\sigma_0 = e^2 \tau_0 \epsilon_F / \pi \hbar^2$  is the conductivity in the absence of spin-orbit coupling. Interestingly, the Rashba-induced torque ( $\propto \alpha$ ) only depends on the relative angle between the magnetization and the electric field ( $\theta - \theta_0$ ), whereas the Dresselhaus-induced torque ( $\propto \beta$ ) depends on the absolute angles ( $\theta + \theta_0$ ). This comes from the specific form of the Dresselhaus coupling: whereas Rashba SOI arises from the structure asymmetry, namely, the lack of symmetry between the top and bottom interfaces, the Dresselhaus effect comes from the lack of symmetry of the crystal itself. Consequently, the Dresselhaus torque depends on the relative orientation of the magnetization and the electric field with respect to the crystal axes, here  $(x, y)$ , whereas these axes do not play any role in the Rashba torque. Note that these different angular dependences were used by Ganichev *et al.*<sup>27</sup> to separate the Dresselhaus contribution from the Rashba contribution in zero-field spin-splitting studies.

We can also estimate the anomalous Hall effect and anisotropic magnetoresistance. To do so, we make the hypothesis that the electron spin is aligned on the magnetization. We use the formalism developed by Schliemann and Loss<sup>26</sup> and find that the longitudinal and transverse conductivities are

$$\begin{aligned} \sigma_{\parallel} &= \sigma_0 \left[ 1 + \left( \frac{v_D}{v_F} \right)^2 \sin^2(\theta + \theta_0) + \left( \frac{v_R}{v_F} \right)^2 \cos^2(\theta - \theta_0) \right. \\ &\quad \left. - \frac{v_R v_D}{v_F^2} (\sin 2\theta + \sin 2\theta_0) \right], \end{aligned} \quad (51)$$

$$\begin{aligned} \sigma_{\perp} &= \frac{\sigma_0}{2} \left[ \left( \frac{v_D}{v_F} \right)^2 \sin 2(\theta + \theta_0) + \left( \frac{v_R}{\hbar v_F} \right)^2 \sin 2(\theta - \theta_0) \right. \\ &\quad \left. - 2 \frac{v_R v_D}{v_F^2} \cos 2\theta_0 \right], \end{aligned} \quad (52)$$

where  $v_F = \sqrt{2\epsilon_F/m}$  is the Fermi velocity,  $v_R = \alpha/\hbar$ , and  $v_D = \beta/\hbar$ . The corresponding AMR is then

$$\begin{aligned} \text{AMR} &= \frac{\sigma_{\parallel}(\theta = \theta_0 + \pi/2) - \sigma_{\parallel}(\theta = \theta_0)}{\sigma_{\parallel}(\theta = \theta_0)} = \left( \frac{v_D}{v_F} \right)^2 \cos 4\theta_0 \\ &\quad - \left( \frac{v_R}{v_F} \right)^2 + \frac{v_R v_D}{v_F^2} 2 \sin 2\theta_0. \end{aligned} \quad (53)$$

Interestingly, in two-dimensional systems, the AMR is a second-order effect ( $\propto \alpha^2, \beta^2$ ), whereas the spin torque is a first-order mechanism ( $\propto \alpha, \beta$ ). Furthermore, the AMR changes its sign depending whether Rashba or Dresselhaus SOI is stronger. The implications of this dependence on the SOI will be discussed in Sec. IV.

## 2. Weak exchange coupling

Since we are only interested in the lowest-order contribution to the transport, we calculate the torque at the zeroth order in  $s$ - $d$  coupling.<sup>11</sup> This is justified by the fact that the torque is defined as proportional to the  $s$ - $d$  coupling and arises from the scattering anisotropy induced by the spin-orbit coupling. However, we still have to assume either  $\alpha \gg \beta$  or  $\beta \gg \alpha$  in order to find analytical formulas. Then, after developing the energy and scattering matrix up to the zeroth order in  $J_{sd}$ , but up to the first order in either  $\beta$  or  $\alpha$ , we straightforwardly find

$$\mathbf{T} = J_e \frac{J_{sd}}{E_F} \frac{m}{e\hbar} \left( \frac{v_R}{2} \cos(\theta - \theta_0) + v_D \sin(\theta + \theta_0) \right) \mathbf{z}, \quad \beta \gg \alpha, \quad (54)$$

$$\mathbf{T} = J_e \frac{J_{sd}}{E_F} \frac{m}{e\hbar} \left( v_R \cos(\theta - \theta_0) + \frac{v_D}{2} \sin(\theta + \theta_0) \right) \mathbf{z}, \quad \alpha \gg \beta. \quad (55)$$

Consequently, in the weak exchange coupling limit the torque is proportional to  $\lambda_{so}/2$  ( $\lambda_{so} = \alpha, \beta$ ), whereas it is proportional to  $\lambda_{so}$  in the strong exchange coupling limit.

## 3. Cubic Dresselhaus SOI

Now that we have treated  $k$ -linear SOI in 2DEG, we turn ourselves to the case of cubic Dresselhaus SOI. Similarly to the previous calculations, we restrict the electron motion to a two-dimensional plane for simplicity. This restriction simplifies the treatment below and does not fundamentally modify the results. Assuming a spin-orbit Hamiltonian in the form of Eq. (31), we find that the spin density is

$$\begin{aligned} m_x^s &= 2s \left\{ -\cos \theta + \frac{\gamma}{J_{sd}} [\sin^2 \theta k_x (k_y^2 - k_z^2) \right. \\ &\quad \left. - \cos \theta \sin \theta k_y (k_z^2 - k_x^2)] \right\}, \end{aligned} \quad (56)$$

$$m_y^s = -2s \left\{ \sin \theta + \frac{\gamma}{J_{sd}} [\cos \theta \sin \theta k_x (k_y^2 - k_z^2) - \cos^2 \theta k_y (k_z^2 - k_x^2)] \right\}. \quad (57)$$

Then, the corresponding spin torque is

$$T^s = -2s\gamma [\sin \theta k_x (k_y^2 - k_z^2) - \cos \theta k_y (k_z^2 - k_x^2)] \mathbf{z}. \quad (58)$$

The form of the torque is very different from the  $k$ -linear Dresselhaus SOI case and involves symmetric terms ( $k_y^2 - k_z^2$ ) and ( $k_z^2 - k_x^2$ ). Assuming a relaxation-time approximation, we find that the angular summation cancels out due to the isotropy of the interaction;  $\langle k_x^2 \rangle = \langle k_y^2 \rangle = \langle k_z^2 \rangle$ . Then, no net torque exists at the first order with pure cubic Dresselhaus effect. To determine the form of the SOI-induced spin torque in this case, one has to develop the spin density up to the second order at least.

#### IV. DISCUSSIONS

##### A. Role of SOI symmetries

In Sec. III, we obtained two sorts of result: in the case of impurity-induced SOI, cubic Dresselhaus effect and Luttinger spin-orbit, the SOI-induced torque is at least on the order of  $\lambda_{so}^2$ . In contrast, in the case of SIA systems (Rashba and  $k$ -linear Dresselhaus SOIs), the spin torque is on the order of  $\lambda_{so}$ .

The difference between these two types of systems comes from the symmetry of the spin-orbit interaction. In the case of a system with a *spatial inversion symmetry* (impurity-induced SOI and Luttinger SOI),  $V(\mathbf{r}) = V(-\mathbf{r}) \Rightarrow H_{so}(\mathbf{r}) = H_{so}(-\mathbf{r})$  and the spin torque is found to be zero at the first order. In the case of cubic Dresselhaus SOI, although the interaction possesses a BIA,  $H_{so}(\mathbf{k}) = -H_{so}(-\mathbf{k})$ , it also possesses a *rotational symmetry* (the SOI is invariant under circular permutations over the  $x, y, z$  indices). In the case of an isotropic environment, the  $\mathbf{k}$  integration vanishes and the spin torque is found to be zero at the first order.

Interestingly, in all these systems,  $AMR \propto \lambda_{so}^2$ .<sup>6</sup> Since, the amplitude of AMR is on the order of a few percent only (in both transition-metal alloys and DMS), the spin torque arising at higher order is expected to be too small to manipulate the magnetization direction of a ferromagnet.

In the case of SIA, the spin-orbit interaction is linear in  $\mathbf{k}$  and depends on its sign, so that  $H_{so}(\mathbf{k}) = -H_{so}(-\mathbf{k})$ . Furthermore, contrary to the three-dimensional cases (impurities, Luttinger, and cubic Dresselhaus),  $H_{so}$  does not depend on the electron position  $\mathbf{r}$ . This implies that the symmetry rules do not apply here and a nonzero torque is found at the first order in  $\lambda_{so}$ . In such systems, the AMR is on the order of  $\lambda_{so}^2$ , which indicates that even if the AMR is only a few percent, the spin torque is expected to be strong enough to control the magnetization for a reasonable current density.

##### B. SOI spin torque versus spin-transfer torque

It is interesting to compare the present spin torque with the conventional spin-transfer torque.<sup>1,2</sup> First of all, the spin-

transfer torque comes from the absorption of the *transverse* spin current by the magnetization and thus it requires a *non-collinear* magnetization configuration in the direction of the spin current (e.g., spin-valve structures or domain walls). The electrical current must flow perpendicular to the plane of the layers. In general, the STT possesses two components, referred to as in plane and out of plane. The former generally dominates the latter and directly competes with the damping torque. Consequently, the STT induces magnetization switching<sup>3</sup> as well as steady high-frequency magnetic precessions.<sup>28</sup> The out-of-plane component of the STT acts as an effective field on the local magnetization and is responsible for current-induced domain-wall motion.<sup>5</sup>

The present SOI-induced spin torque is created by the intrinsic (or extrinsic, in case of impurity-induced SOI) spin-orbit coupling in the nonequilibrium condition and thus it does not involve the transfer of the conduction-electron spin to the magnetization. Then, this torque exists for a uniformly magnetized single layer with the current applied in the plane of the layer and acts as an effective field. Since the torque does not compete with the damping, it cannot excite current-driven steady magnetization precessions, in contrary to the STT.

##### C. Material considerations

As stated in Sec. I, systems showing magnetoresistive effects (metallic spin valves, magnetic tunnel junctions, and magnetic domain walls) all present a STT effect that can be regarded as the reciprocal effect of the magnetoresistance. Consequently, we also expect to observe a spin torque in systems showing AMR effect.

The most promising devices to observe the SOI-induced spin torque are the magnetic 2DEG. In Ref. 11, we estimated that the current density needed to switch the magnetization of a GaMnAs-type 2DEG, assuming  $\alpha = 10^{-11}$  eV m, would be about  $5 \times 10^6$  A/cm<sup>2</sup>. Depending on the material characteristics (SOI strength, carrier effective mass, carrier density, etc.), the critical current is expected to be on the order of  $10^4 - 10^6$  A/cm<sup>2</sup>.

The relative amplitude of Rashba and Dresselhaus SOIs has been studied experimentally. Since the linear Dresselhaus SOI arises from mechanical strains in the layers, the ratio depends on the material. Then, ratios  $\alpha/\beta \approx 1-7$  have been measured.<sup>29</sup> As an example, Miller *et al.*<sup>25</sup> measured the three contributions of SOI in a GaAs/AlGaAs 2DEG:  $\alpha = 4 \times 10^{-13}$  eV m,  $\beta = 5 \times 10^{-13}$  eV m, and  $\gamma = 3 \times 10^{-29}$  eV m<sup>3</sup>. Furthermore, Rashba spin-orbit coupling on the order of  $10^{-11}$  eV m has been found in InGaAs/In<sub>0.77</sub>Ga<sub>0.23</sub>As (Ref. 30) and in HgCdTe.<sup>31</sup> One would expect that the Rashba parameter should be similar for the Mn-doped dilute magnetic semiconductors in the quantum wells.<sup>32</sup>

Besides conventional semiconductor 2DEG, SOI-induced spin splitting has been studied at nonmagnetic metallic surfaces, where only Rashba SOI is present. Heavy-metal interfaces<sup>33</sup> have shown Rashba SOI on the order of  $10^{-11}$  eV m or above. Very few experimental studies have been published on magnetic interfaces, but recent investiga-

tions suggest strong Rashba SOI in such systems also.<sup>34</sup> Strong spin-orbit coupling due to the presence of interfacial oxide has also been reported<sup>35,36</sup> and could lead to significant Rashba interactions.

The last system that may provide interesting results regarding the SOI-induced torque is the conductive interface formed between two insulating oxides. The electronic reconstruction at the interface between two dielectric perovskites, such as  $\text{LaAlO}_3/\text{SrTiO}_3$  (Ref. 37) or  $\text{LaTiO}_3/\text{SrTiO}_3$ ,<sup>38</sup> creates high-mobility quasi-two-dimensional electron gas (q2-DEG). This gas is generated through different mechanisms depending on the structure: electron transfer between one sublattice to another,<sup>39</sup> oxygen vacancies, or polarity discontinuity<sup>38</sup> between the two perovskite insulators. This suggests the presence of a sharp potential gradient<sup>40</sup> that produces electrons in excess at the interface. This potential gradient could be asymmetrically designed in order to obtain a large Rashba effective interaction. The recent demonstration of ferromagnetism at  $\text{LaAlO}_3/\text{SrTiO}_3$  interfaces<sup>41</sup> is of great interest for the present study, providing magnetic 2q-DEG with tunable Rashba SOI.

## V. CONCLUSION

The combined effect of spin-orbit coupling and exchange interaction has been theoretically studied in a single homogeneous ferromagnetic layer. We showed that, in principle, the spin-dependent scattering arising from the spin-orbit coupling induces an out-of-equilibrium spin density when applying an external current. This spin density can be used to manipulate the magnetization direction of the layer, without the use of an additional polarizing layer.

We then addressed the form of this torque considering several forms of the spin-orbit coupling. In the presence of impurities, we find that the spin torque is present only at higher order in spin-orbit coupling due to the symmetry of the interaction. Consequently, we expect a critical switching current larger than the one needed with the conventional STT ( $>10^7$  A/cm<sup>2</sup>).

In DMS, the transport is represented by a Luttinger Hamiltonian and the spin-orbit arises from the band structure itself. Again, due to the symmetry of the interaction, the spin torque effect does not exist at the first order.

In systems showing linear spin-orbit interaction, such as Rashba and Dresselhaus SOIs, the spin torque is on the first order in SOI. The magnetization direction can be controlled by the electrical current, using critical current densities on the order of  $10^4$ – $10^6$  A/cm<sup>2</sup>. The cubic Dresselhaus spin-orbit coupling does not generate a spin torque at the first order.

We finally discussed the possibility of observing the SOI-induced spin torque in a number of systems, including metallic and semiconductor-based magnetic 2DEG and oxide interfaces. Up to now, the experimental studies have mainly addressed the characteristics of Rashba SOI in nonmagnetic 2DEG, but the recent realization of magnetic 2DEG using DMS (Ref. 32) or oxide interfaces<sup>41</sup> constitutes a promising step toward the observation of the SOI-induced spin torque.

## ACKNOWLEDGMENTS

This work was supported by NSF (Contract No. DMR-0704182) and DOE (Contract No. DE-FG02-06ER46307).

<sup>1</sup>J. C. Slonczewski, *J. Magn. Magn. Mater.* **159**, L1 (1996).

<sup>2</sup>L. Berger, *Phys. Rev. B* **54**, 9353 (1996).

<sup>3</sup>J. A. Katine, F. J. Albert, R. A. Buhrman, E. B. Myers, and D. C. Ralph, *Phys. Rev. Lett.* **84**, 3149 (2000).

<sup>4</sup>Y. Huai, F. Albert, P. Nguyen, M. Pakala, and T. Valet, *Appl. Phys. Lett.* **84**, 3118 (2004); G. D. Fuchs, N. C. Emley, I. N. Krivorotov, P. M. Braganca, E. M. Ryan, S. I. Kiselev, J. C. Sankey, D. C. Ralph, R. A. Buhrman, and J. A. Katine, *ibid.* **85**, 1205 (2004).

<sup>5</sup>M. Klaui, C. A. F. Vaz, J. A. C. Bland, W. Wernsdorfer, G. Faini, E. Cambril, and L. J. Heyderman, *Appl. Phys. Lett.* **83**, 105 (2003).

<sup>6</sup>T. R. McGuire and R. I. Potter, *IEEE Trans. Magn.* **11**, 1018 (1975); O. Jaoul, I. A. Campbell, and A. Fert, *J. Magn. Magn. Mater.* **5**, 23 (1977).

<sup>7</sup>N. Nagaosa, *J. Phys. Soc. Jpn.* **75**, 042001 (2006).

<sup>8</sup>J. E. Hirsch, *Phys. Rev. Lett.* **83**, 1834 (1999).

<sup>9</sup>A. K. Nguyen, H. J. Skadsem, and A. Brataas, *Phys. Rev. Lett.* **98**, 146602 (2007).

<sup>10</sup>K. Obata and G. Tatara, *Phys. Rev. B* **77**, 214429 (2008).

<sup>11</sup>A. Manchon and S. Zhang, *Phys. Rev. B* **78**, 212405 (2008).

<sup>12</sup>Y. A. Bychkov and E. I. Rashba, *J. Phys. C* **17**, 6039 (1984).

<sup>13</sup>G. Dresselhaus, *Phys. Rev.* **100**, 580 (1955).

<sup>14</sup>J. Smit, *Physica (Amsterdam)* **21**, 877 (1955); **24**, 39 (1958); S. K. Lyo and T. Holstein, *Phys. Rev. Lett.* **29**, 423 (1972).

<sup>15</sup>L. Berger, *Phys. Rev. B* **2**, 4559 (1970); **5**, 1862 (1972).

<sup>16</sup>A. Crepieux and P. Bruno, *Phys. Rev. B* **64**, 014416 (2001).

<sup>17</sup>R. C. Fivaz, *Phys. Rev.* **183**, 586 (1969).

<sup>18</sup>R. I. Potter, *Phys. Rev. B* **10**, 4626 (1974).

<sup>19</sup>H. Ohno, *Science* **281**, 951 (1998).

<sup>20</sup>T. Dietl, *J. Phys. Soc. Jpn.* **77**, 031005 (2008); T. Jungwirth, J. Sinova, J. Masek, J. Kueera, and A. H. MacDonald, *Rev. Mod. Phys.* **78**, 809 (2006).

<sup>21</sup>J. M. Luttinger, *Phys. Rev.* **102**, 1030 (1956).

<sup>22</sup>M. Abolfath, T. Jungwirth, J. Brum, and A. H. MacDonald, *Phys. Rev. B* **63**, 054418 (2001).

<sup>23</sup>G. C. La Rocca, N. Kim, and S. Rodriguez, *Phys. Rev. B* **38**, 7595 (1988); M. I. Dyakonov and V. Y. Kachorovskii, *Sov. Phys. Semicond.* **20**, 110 (1986).

<sup>24</sup>M. Kohda, T. Bergsten, and J. Nitta, *J. Phys. Soc. Jpn.* **77**, 031008 (2008).

<sup>25</sup>J. B. Miller, D. M. Zumbuhl, C. M. Marcus, Y. B. Lyanda-Geller, D. Goldhaber-Gordon, K. Campman, and A. C. Gossard, *Phys. Rev. Lett.* **90**, 076807 (2003).

<sup>26</sup>J. Schliemann and D. Loss, *Phys. Rev. B* **68**, 165311 (2003).

<sup>27</sup>S. D. Ganichev, V. V. Belkov, L. E. Golub, E. L. Ivchenko, P.



- Schneider, S. Giglberger, J. Eroms, J. De Boeck, G. Borghs, W. Wegscheider, D. Weiss, and W. Prettl, *Phys. Rev. Lett.* **92**, 256601 (2004).
- <sup>28</sup>S. I. Kiselev, J. C. Sankey, I. N. Krivorotov, N. C. Emley, R. J. Schoelkopf, R. A. Buhrman, and D. C. Ralph, *Nature (London)* **425**, 380 (2003).
- <sup>29</sup>S. Giglberger, L. E. Golub, V. V. Belkov, S. N. Danilov, D. Schuh, C. Gerl, F. Rohlfing, J. Stahl, W. Wegscheider, D. Weiss, W. Prettl, and S. D. Ganichev, *Phys. Rev. B* **75**, 035327 (2007); A. V. Larionov and L. E. Golub, *ibid.* **78**, 033302 (2008); M. Akabori, V. A. Guzenko, T. Sato, Th. Schapers, T. Suzuki, and S. Yamada, *ibid.* **77**, 205320 (2008).
- <sup>30</sup>Y. Sato, T. Kita, S. Gozu, and S. Yamada, *J. Appl. Phys.* **89**, 8017 (2001).
- <sup>31</sup>J. Hinz, H. Buhmann, M. Schafer, V. Hock, C. R. Becker, and L. W. Molenkamp, *Semicond. Sci. Technol.* **21**, 501 (2006).
- <sup>32</sup>A. Bove, F. Altomare, N. B. Kundtz, Albert M. Chang, Y. J. Cho, X. Liu, and J. Furdyna, arXiv:0802.3863 (unpublished); F. J. Teran, M. Potemski, D. K. Maude, Z. Wilamowski, A. K. Hassan, D. Plantier, J. Jaroszynski, T. Wojtowicz, and G. Karcewski, *Physica E* **17**, 335 (2003).
- <sup>33</sup>S. LaShell, B. A. McDougall, and E. Jensen, *Phys. Rev. Lett.* **77**, 3419 (1996); H. Cercellier, C. Didiot, Y. Fagot-Revurat, B. Kirerren, L. Moreau, D. Malterre, and F. Reinert, *Phys. Rev. B* **73**, 195413 (2006); C. R. Ast, J. Henk, A. Ernst, L. Moreschini, M. C. Falub, D. Pacilé, P. Bruno, K. Kern, and M. Grioni, *Phys. Rev. Lett.* **98**, 186807 (2007).
- <sup>34</sup>O. Krupin, G. Bihlmayer, K. Starke, S. Gorovikov, J. E. Prieto, K. Dobrich, S. Blugel, and G. Kaindl, *Phys. Rev. B* **71**, 201403(R) (2005).
- <sup>35</sup>L. Gao, X. Jiang, S.-H. Yang, J. D. Burton, E. Y. Tsybal, and S. S. P. Parkin, *Phys. Rev. Lett.* **99**, 226602 (2007); A. N. Chantis, K. D. Belashchenko, E. Y. Tsybal, and M. van Schilfgaarde, *ibid.* **98**, 046601 (2007).
- <sup>36</sup>A. Manchon, S. Pizzini, J. Vogel, V. Uhler, L. Lombard, C. Ducruet, S. Auffret, B. Rodmacq, B. Dieny, M. Hochstrasser, and G. Panaccione, *J. Appl. Phys.* **103**, 07A912 (2008); B. Rodmacq, A. Manchon, C. Ducruet, S. Auffret, and B. Dieny, *Phys. Rev. B* **79**, 024423 (2009).
- <sup>37</sup>A. Ohtomo and H. Y. Hwang, *Nature (London)* **427**, 423 (2004).
- <sup>38</sup>S. Thiel, G. Hammerl, A. Schmehl, C. W. Schneider, and J. Mannhart, *Science* **313**, 1942 (2006).
- <sup>39</sup>A. Ohtomo, D. A. Muller, J. L. Grazul, and H. Y. Hwang, *Nature (London)* **419**, 378 (2002).
- <sup>40</sup>Z. S. Popovic and S. Satpathy, *Phys. Rev. Lett.* **94**, 176805 (2005).
- <sup>41</sup>A. Brinkman, M. Huijben, M. Van Zalk, J. Huijben, U. Zeitler, J. C. Maan, W. G. Van Der Wiel, G. Rijnders, D. H. A. Blank, and H. Hilgenkamp, *Nature Mater.* **6**, 493 (2007).